38th International Electric Vehicle Symposium and Exhibition (EVS38)
Göteborg, Sweden, June 15-18, 2025

Road Friction Coefficient Estimation for Non-pneumatic Tire using Cubature Kalman filter and Multilayer Perceptron

DongWook Cho[1], Hyunuk Lee[1], Jeonghyuk Kim[2], Jiwon Im[2], Sung-Ho Hwang[2]
[1]*Department of Intelligent Robotics, Sungkyunkwan University, Republic of Korea, dw0313@g.skku.edu*
[2]*Department of Mechanical Engineering, Sungkyunkwan University, Republic of Korea*

Executive Summary

Recent advancements in non-pneumatic tires (NPT) have highlighted their practical advantages over conventional pneumatic tires, such as eliminating air pressure management and reducing puncture risks. This study presents a modeling and estimation framework for NPT by optimizing a modified Magic Formula tire model using a Genetic Algorithm (GA) based on reference tire data. A vehicle dynamics simulator, CarMaker, was employed to simulate general driving scenarios and validate the modeled tire forces within a four-wheel vehicle model. An additional Multi-Layer Perceptron (MLP) network was developed to estimate the tire-road friction coefficient (TRFC) using estimated tire forces, slip angles, and slip ratios. Simulation results show accurate TRFC and vehicle state estimations under high-friction conditions, with moderate performance degradation under low-friction environments. The proposed approach provides an efficient simulation-based methodology for advancing the development and control of NPT-equipped vehicles.

Keywords: AI-Artificial intelligence for EVs, Modelling & Simulation, Vehicle Motion & Stability Control, Electric Vehicles

1 Introduction

Non-pneumatic tires (NPT) are gaining increasing attention as alternatives to conventional pneumatic tires, offering freedom from the need to maintain air pressure and eliminating the risk of punctures. NPT maintain consistent performance irrespective of air pressure variations, which is a critical factor in enhancing vehicle safety and operational efficiency. While previous studies have primarily focused on structural analyses and component-level force measurements of NPT under pure slip conditions[1, 2], research on assessing NPT performance through full-vehicle dynamic simulations remains limited.
In parallel, accurate vehicle state estimation has been recognized as essential for ensuring vehicle stability, safety, and control performance. Among various state variables, the tire-road friction coefficient (TRFC) plays a crucial role in influencing vehicle dynamics and control strategies. Consequently, reliable TRFC estimation has become a major research focus in the field of automotive engineering.
Existing TRFC estimation methods can be broadly categorized into three main approaches: observer-based methods, nonlinear Kalman filter-based methods, and data-driven methods[3]. Observer-based methods estimate TRFC indirectly by reconstructing tire forces, whereas nonlinear Kalman filters such

as the Unscented Kalman Filter (UKF) and Cubature Kalman Filter (CKF) enhance estimation robustness by fusing sensor measurements with vehicle dynamic models[4, 5]. Data-driven methods, such as those proposed by Tao et al.[6], utilize neural networks trained on observer-estimated tire forces to infer TRFC. Recently, hybrid approaches that combine model-based estimation with data-driven learning have been increasingly explored. Bei et al.[7] introduced a framework that integrates CKF-based state estimation with Magic Formula-based tire force modeling to generate normalized data for training neural networks, thereby improving TRFC estimation across varying conditions. Such hybrid methods have gained attention as they outperform traditional approaches based solely on observers, filters, or physical models by leveraging the complementary strengths of physical modeling and machine learning.
Despite these advancements, most TRFC estimation research has assumed the use of conventional pneumatic tires. Given the distinct force-slip characteristics of NPT compared to pneumatic tires, there is a critical need to adapt TRFC estimation frameworks to accommodate the specific behaviors of NPT. Reliable estimation of TRFC for NPT-equipped vehicles is vital not only for performance validation but also for ensuring driving safety in future applications.
Therefore, this study addresses NPT and proposes a framework for optimizing an NPT tire model using the Magic Formula and estimating the normalized tire-road friction coefficient during dynamic driving scenarios. This integrated approach aims to validate the driving performance of NPT-equipped vehicles through full-vehicle simulations, ultimately contributing to the safer and more efficient design of non-pneumatic tires.

2 Modeling

2.1 Vehicle Model

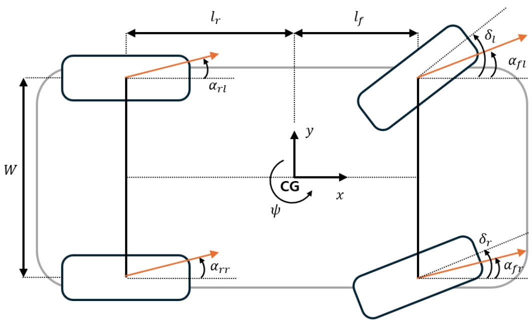

Figure 1: Schematic diagram of planar vehicle

A nonlinear 3-degree-of-freedom (3DOF) vehicle model, which includes longitudinal, lateral, and yaw motions, is considered. The equations below represent the longitudinal, lateral, and yaw dynamics of the vehicle.

$$\dot{v}_x = \frac{1}{m}\left((F_{xfl} + F_{xfr})\cos\delta - (F_{yfl} + F_{yfr})\sin\delta + (F_{xrl} + F_{xrr}) - C_A v_x^2\right) \tag{1}$$

$$\dot{v}_y = \frac{1}{m}\left((F_{xfl} + F_{xfr})\sin\delta + (F_{yfl} + F_{yfr})\cos\delta + (F_{xrl} + F_{xrr})\right) \tag{2}$$

$$
\begin{aligned}
\dot{\gamma} = \frac{1}{I_{zz}} \Bigg[& l_f \left((F_{xfl} + F_{xfr}) \sin\delta + (F_{yfl} + F_{yfr}) \cos\delta \right) \\
& - \frac{W}{2}(F_{xfl}\cos\delta - F_{xfr}\sin\delta) + \frac{W}{2}(F_{yfl}\sin\delta - F_{yfr}\sin\delta) \\
& - \frac{W}{2}(F_{xrl} - F_{xrr}) - l_r(F_{yrl} - F_{yrr}) \Bigg]
\end{aligned} \tag{3}
$$

The variables used in the above equations are defined as follows: m denotes the vehicle mass, and δ represents the steering angle of the front wheels. v_x and v_y are the longitudinal and lateral velocities of the vehicle, respectively, while γ means the yaw rate. l_f and l_r indicate the distances from the vehicle's center of gravity to the front and rear axles, respectively. W denotes the wheel tread, and I_{zz} is the moment of inertia about the vertical z-axis. F_{xij} and F_{yij} are the longitudinal and lateral tire forces, respectively, where $ij = [fl, fr, rl, rr]$ denotes the front-left, front-right, rear-left, and rear-right wheels.

2.2 Magic Formula Tire Model

The Magic Formula tire model[8] is a representative empirical model widely used to describe the force characteristics of pneumatic tires. In this study, it was adopted to investigate its applicability to NPT, even though it was originally developed for pneumatic applications.

$$
y_0 = D \sin\left[C \arctan\left\{Bx - E\left(Bx - \arctan\left(Bx\right)\right)\right\}\right] + S_V \tag{4}
$$

$$
F_{x0} = \frac{\mu}{\mu_0} y_{x0} \left(\frac{\mu_0}{\mu} \lambda \right), \; F_{y0} = \frac{\mu}{\mu_0} y_{y0} \left(\frac{\mu_0}{\mu} \alpha \right) \tag{5}
$$

The general form of the Magic Formula tire force can be expressed as y_0, which holds the same structure for both longitudinal and lateral directions. The pure longitudinal and lateral tire forces are denoted as F_x and F_y, respectively. When the actual tire-road friction coefficient is represented by μ, the normalized friction coefficient is denoted as μ_0. In this study, the normalized tire force was utilized as a basis for estimating the actual tire-road friction coefficient μ. For this purpose, the normalized reference value was set to $\mu_0 = 1$, assuming a fully saturated friction condition.

The equations used to compute the vertical load are given as follows:

$$
\begin{cases}
F_{zfj} = F_{zfj[\text{nominal}]} - \dfrac{m a_x h_{cg}}{2(l_f + l_r)} \mp \dfrac{m a_y h_{cg}}{W} \cdot \dfrac{l_r}{l_f + l_r} \\
F_{zrj} = F_{zrj[\text{nominal}]} + \dfrac{m a_x h_{cg}}{2(l_f + l_r)} \mp \dfrac{m a_y h_{cg}}{W} \cdot \dfrac{l_f}{l_f + l_r}
\end{cases} \tag{6}
$$

h_{cg} means height of the center of gravity of vehicle.

Tire slip angle can be calculated as follows:

$$
\begin{cases}
\alpha_{fl} = \arctan\left(\dfrac{v_y + l_f \gamma}{v_x - W\gamma/2} \right) - \delta_l \\
\alpha_{fr} = \arctan\left(\dfrac{v_y + l_f \gamma}{v_x + W\gamma/2} \right) - \delta_r \\
\alpha_{rl} = \arctan\left(\dfrac{v_y - l_r \gamma}{v_x - W\gamma/2} \right) \\
\alpha_{rr} = \arctan\left(\dfrac{v_y - l_r \gamma}{v_x + W\gamma/2} \right)
\end{cases} \tag{7}
$$

Tire slip ratio can be determined by:

$$\lambda_{ij} = \begin{cases} \dfrac{R_e\omega_{ij} - v_{xij}}{v_{xij}}, & (v_{xij} \neq 0 \text{ or } \omega_{ij} \neq 0) \\ 0, & (v_{xij} = \omega_{ij} = 0) \end{cases} \tag{8}$$

where R_e is the effective rolling tire radius, w_{ij} and v_{xij} are angular velocity of each wheel and longitudinal velocity of each wheel's roll center, respectively.

3 Optimizing NPT with Modified Magic Formula Tire Model

The Genetic Algorithm(GA) was also selected as the global optimization algorithm to enhance the diversity of solutions and search capabilities.

3.1 Magic Formula Tire Model

We utilized the Magic Formula tire model to model NPT, referencing data from Laiyun Ku[2]. Additionally, to reflect the reduced forces at the same vertical load compared to pneumatic tires, we introduced parameters PDX3 and PDY4. Figure 2 compares pneumatic and non-pneumatic tires under a vertical load of 4000N. The additional parameters are as follows:

$$F^*_{x0} = F^*_{x0} \cdot PDX3, \quad F^*_{y0} = F^*_{y0} \cdot PDY4 \tag{9}$$

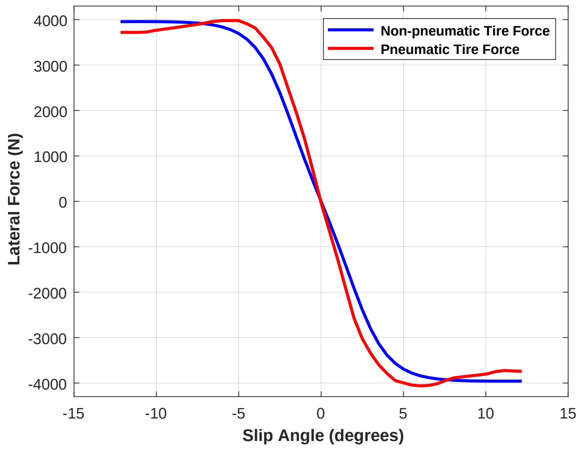

Figure 2: Pneumatic Tire vs Non-pneumatic Tire (Fz=4000N, μ=1.0)

The reference tire data were obtained from a test conducted on a road surface with a friction coefficient of 0.7 at a driving speed of 60 km/h. The corresponding vertical loads were 2000 N, 3500 N, and 5000 N. For lateral force modeling, only the data acquired under a camber angle of 0° were considered as a reference. To improve optimization efficiency and generalization performance under a limited number of data samples, the following two assumptions were made for the parameter optimization:

1. The force characteristics of the NPT pass through the origin.
2. The force characteristics of the NPT are symmetric with respect to the origin.

$$\min \sum_{i=1}^{n} \sum_{j=1}^{m} \left(F_{x0}^{MagicFormula}(X, \lambda_j, F_{zi}) - F_{x0}^{Reference}(\lambda_j, F_{zi}) \right)^2 \tag{10}$$

$$\min \sum_{i=1}^{n} \sum_{j=1}^{m} \left(F_{y0}^{MagicFormula}(Y, \alpha_j, F_{zi}) - F_{y0}^{Reference}(\alpha_j, F_{zi}) \right)^2 \tag{11}$$

The optimization problem was defined as follows: for the longitudinal direction, parameters, slip ratio, and vertical load were set as input variables; for the lateral direction, parameters, slip angle, and vertical load were set as input variables. The objective was to minimize the squared sum of the differences between the reference data and the Magic Formula tire model. The GA parameters are in the table below.

Table 1: Parameters of Genetic Algorithm (GA)

Parameters	**Value**
Number of Population (NP)	1000
Number of parameters to optimize (D)	16 (Longitudinal), 15 (Lateral)
Crossover Probability (CP)	0.4
Mutation Probability (MP)	0.1
Number of iterations (itermax)	10000

4 TRFC estimation

4.1 Vehicle state estimation using CKF

To estimate the longitudinal and lateral velocities as well as the yaw rate of the vehicle during driving, a Cubature Kalman Filter (CKF) [9], a type of nonlinear Kalman filter, was employed. The measurement vector was defined as $z_k = [a_x(k), a_y(k), \gamma(k)]^T$, and the state vector was set as $x_k = [v_x(k), v_y(k), \gamma(k)]^T$.

Algorithm 1: CKF Iteration

Inputs: Prior state estimate $\hat{x}_{k-1|k-1}$, covariance $P_{k-1|k-1}$, process noise Q_{k-1}, measurement noise R_{k-1}, control input u_{k-1}, measurement z_k, auxiliary variable: $\zeta_i = \sqrt{n}[I_n, -I_n]_i,\ i = 1, 2, \cdots, 2n$

Time Update (Prediction)

1) *Evaluate the cubature points:*
$S_{k-1} = \sqrt{P_{k-1|k-1}}$
$X_{i,k-1|k-1} = \hat{x}_{k-1|k-1} + S_{k-1}\xi_i$
2) *Evaluate cubature points:*
$X^*_{i,k|k-1} = f(X_{i,k-1|k-1}, u_{k-1})$
3) *Estimate the predicted state:*
$\hat{x}_{k|k-1} = \frac{1}{2n}\sum_{i=1}^{2n} X^*_{i,k|k-1}$
4) *Estimate the error covariance:*
$$P_{k|k-1} = \frac{1}{2n}\sum_{i=1}^{2n} X^*_{i,k|k-1}X^{*T}_{i,k|k-1} - \hat{x}_{k|k-1}\hat{x}^T_{k|k-1} + Q_{k-1}$$

Measurement Update (Correction)

1) *Evaluate the cubature points:*
$S_{k|k-1} = \sqrt{P_{k|k-1}}$
$X_{i,k|k-1} = \hat{x}_{k|k-1} + S_{k|k-1}\xi_i$
2) *Evaluate cubature points:*
$Z_{i,k|k-1} = h(X_{i,k|k-1}, u_{k-1})$
3) *Estimate the predicted measurement:*
$\hat{z}_{k|k-1} = \frac{1}{2n}\sum_{i=1}^{2n} Z_{i,k|k-1}$
4) *Estimate the innovation covariance:*
$$P_{zz,k|k-1} = \frac{1}{2n}\sum_{i=1}^{2n} Z_{i,k|k-1}Z^T_{i,k|k-1} - \hat{z}_{k|k-1}\hat{z}^T_{k|k-1} + R_k$$
5) *Estimate the cross-covariance:*
$P_{xz,k} = \frac{1}{2n}\sum_{i=1}^{2n} X_{i,k|k-1}Z^T_{i,k|k-1} - \hat{x}_{k|k-1}\hat{z}^T_{k|k-1}$

6) *Calculate the Kalman gain:* $K_k = P_{xz,k|k-1}P^{-1}_{zz,k|k-1}$
7) *Update the state estimate:* $\hat{x}_{k|k} = \hat{x}_{k|k-1} + K_k(z_k - \hat{z}_{k|k-1})$
8) *Update the error covariance:* $P_{k|k} = P_{k|k-1} - K_k P_{zz,k} K^T_k$

4.2 TRFC estimation with Multi-Layer Perceptron(MLP)

4.2.1 Data Acquisition and Preprocessing

To generate the tire force dataset, simulation-based driving scenarios were designed considering representative road surface conditions. The tire-road friction coefficient μ was set to five typical values corresponding to different road types: 0.2 (snowy road), 0.4 (cobblestone), 0.6 (wet asphalt), 0.8 (dry asphalt), and 1.0 (high-grip surface), as commonly reported in the literature[10]. For each μ condition, driving maneuvers were simulated at vehicle speeds of 20, 40, 60, and 80 km/h. Each maneuver involved maintaining straight-line driving for 7 seconds, followed by sequential left and right steering operations, with the steering wheel angle increased in steps of $50°$ up to a maximum of $\pm 500°$.
During these maneuvers, the longitudinal force F_x, lateral force F_y, vertical load F_z, slip angle α, and slip ratio λ were recorded. In particular, normalized tire forces (F_{x0} and F_{y0}) based on the reference condition of $\mu_0 = 1.0$ were used to decouple the tire-road friction effects from the force measurements.
Prior to model training, a data preprocessing step was applied to improve the robustness of the learning process. Given that non-pneumatic tires exhibit larger force prediction errors at low slip conditions and that low excitation levels hinder the ability to distinguish meaningful relationships, samples with absolute slip angle or slip ratio less than 0.015 were excluded from the training dataset. This filtering process ensures that the model focuses on regions where the excitation is sufficient to capture the characteristic force-slip behavior. This dataset construction and preprocessing strategy enables comprehensive learning of the relationships among normalized forces, slip characteristics, and vertical loads, without relying on extensive real-world testing.

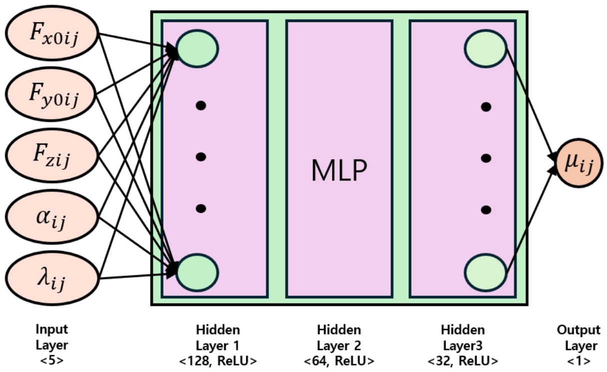

Figure 3: Structure of the MLP model for tire-road friction coefficient (TRFC)

The MLP architecture consists of three hidden layers with 128, 64, and 32 neurons, respectively, each using the ReLU activation function. The final output layer produces a single continuous value corresponding to the estimated TRFC.
Training was conducted using the mean squared error (MSE) loss function and the Adam optimizer with an initial learning rate of 0.0005. An adaptive learning rate strategy was applied, increasing the learning rate by 1.01 when the validation loss decreased and decreasing it by 0.99 otherwise. A batch size of 256 was used, and early stopping with a patience of 30 epochs was implemented to prevent overfitting.
The model was selected based on the best validation loss and evaluated using a threshold-based accuracy metric, considering predictions correct if the absolute error was within 0.05. Finally, the trained MLP was exported to the ONNX format for integration into the CarMaker/Simulink simulation environment.

5 Results and discussion

To validate the proposed estimation algorithm, simulations were conducted in the CarMaker/Simulink environment. The reference data, originally obtained under pure slip conditions, were converted into the TYDEX format and incorporated into the simulation. Due to the absence of experimental combined slip data, the combined slip behavior was reproduced within the simulation environment based on the TYDEX-formatted NPT pure slip data.

5.1 Optimization results of NPT

Since the camber angle was set to zero, the parameters influenced by camber effects, as well as those related to horizontal and vertical shifts around the origin, were fixed at zero and excluded from the optimization process. Figures 4 and 5 compare the reference data and the optimization results of the non-pneumatic tire (NPT) obtained using GA under pure slip conditions. The solid line in these figures denotes the reference tire data, whereas the dashed line denotes the tire data resulting from the optimization process.

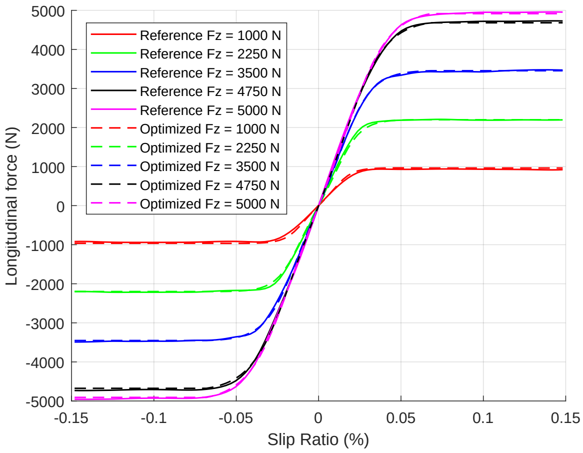

Figure 4: Optimized vs Reference Data : pure longitudinal (μ=1.0)

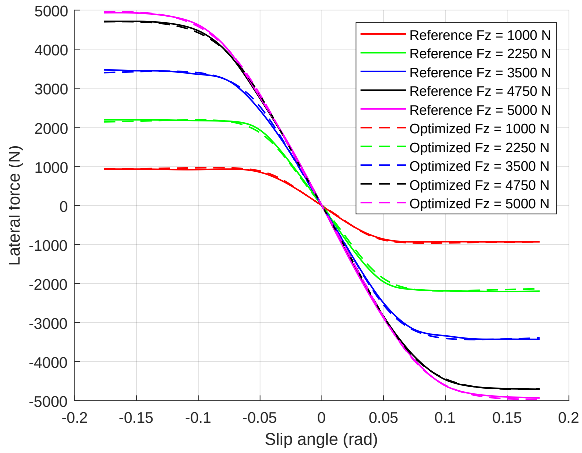

Figure 5: Optimized vs Reference Data : pure lateral (μ=1.0)

Table 2: Optimized coefficients of Magic Formula Tire Model

PCX1	PDX1	PDX2	PEX1	PEX2	PEX3	PEX4	PKX1	PKX2	PKX3
1.1288	0.9987	0.0261	-3.6586	0.5851	-0.3247	-0.0174	32.4583	-4.6262	0.3158
PHX1	PHX2	PVX1	PVX2	PDX3					
0	0	0	0	0.9835					
PCY1	PDY1	PDY2	PDY3	PDY4	PEY1	PEY2	PEY3	PEY4	PKY1
1.2514	1.2035	0.0249	0	0.8118	-3.1349	-0.4670	-0.0331	0	-24.4979
PKY2	PKY3	PHY1	PHY2	PHY3	PVY1	PVY2	PVY3	PVY4	
1.8913	0	0	0	0	0	0	0	0	

The details of the optimized tire parameters are listed in Table 2.

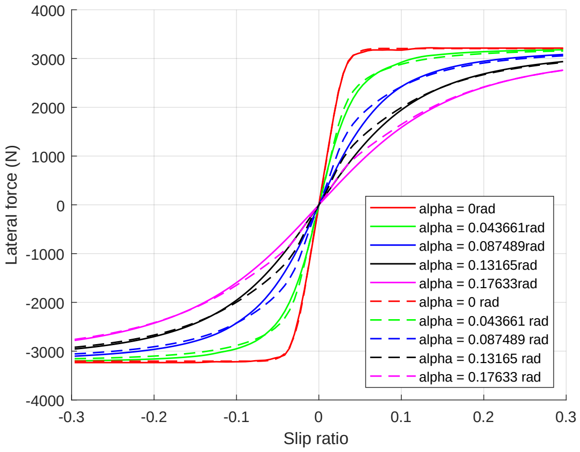

Figure 6: Optimized vs Reference Data : combined longitudinal (Fz=4250N, μ=1.0)

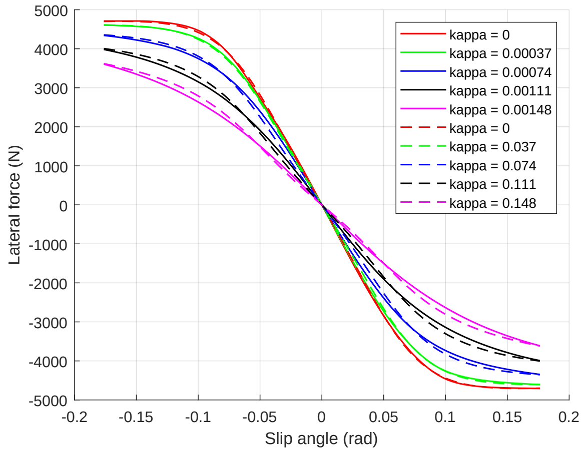

Figure 7: Optimized vs Reference Data : combined lateral (Fz=4250N, μ=1.0)

Figures 6 and 7 present the optimization results obtained under combined slip conditions. The deviations from the reference data are slightly larger compared to those observed under pure slip conditions. This discrepancy may be attributed not only to the inherent limitations of the Magic Formula in modeling coupled slip dynamics, but also to the fundamental differences in force curvature characteristics between pneumatic and non-pneumatic tires (NPT). While conventional pneumatic tires exhibit a gradual decrease in force beyond the peak point, NPT tend to maintain their force levels even after the peak, resulting in a distinct force-slip relationship. Since the Magic Formula is an empirical model originally designed to capture the curvature behavior of pneumatic tires, it may not fully represent the force characteristics of NPT, particularly under low slip ratio and slip angle conditions. Additionally, it was observed that the fitting accuracy tended to degrade in low slip regions, where the force magnitudes were relatively small or large, leading to noticeable deviations from the reference data.

In future work, incorporating combined slip terms into the optimization objective and refining the model to better account for the deformation behavior unique to NPT could further improve the fitting accuracy across a wider range of slip conditions.

5.2 TRFC estimation performance

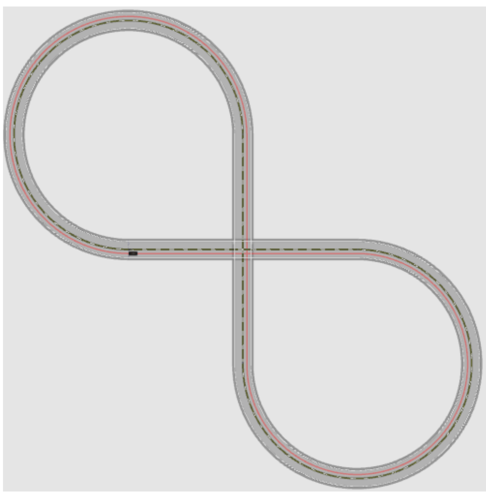

Figure 8: Test track configuration used for TRFC estimation validation

The performance of the TRFC estimation was validated using the CarMaker/Simulink simulation platform. The test scenario involved a track composed of alternating straight and curved sections. Straight sections measured 100 meters in length, and curved sections featured a 50-meter radius with a 270-degree arc. To evaluate performance across different surface conditions, simulations were performed under both high-mu ($\mu = 0.8$) and low-mu ($\mu = 0.4$) settings. The following results present the estimated states and tire forces for the front-left (FL) wheel.

Table 3: Test Vehicle Parameters

Parameters	**Value**
Vehicle Mass (m)	1360 kg
Distance to Front Axle (l_f)	0.983 m
Distance to Rear Axle (l_r)	1.597 m
Track Width (W)	1.470 m
Height of Center of Gravity (h_{cg})	0.531 m
Yaw Moment of Inertia (I_{zz})	1782.008 kg·m^2

The specifications of the test vehicle used for validation are summarized in Table 3.

5.2.1 Case 1: High-mu ($\mu = 0.8$) test results

The vehicle was driven at a target speed of 60 km/h on a track composed of straight and curved sections under a high-mu surface ($\mu = 0.8$). Figures 9–12 present the estimation results for longitudinal and lateral velocities, yaw rate, tire forces, and TRFC.

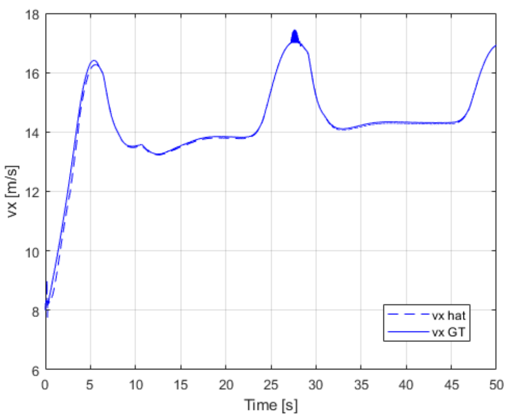

Figure 9: Longitudinal velocity(Vx) estimation (μ=0.8)

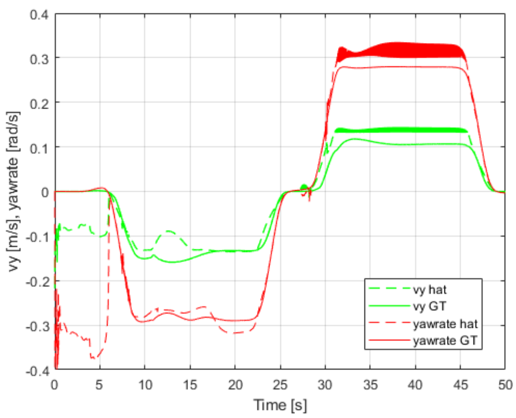

Figure 10: Lateral velocity(Vy) and yawrate(γ) etimation (μ=0.8)

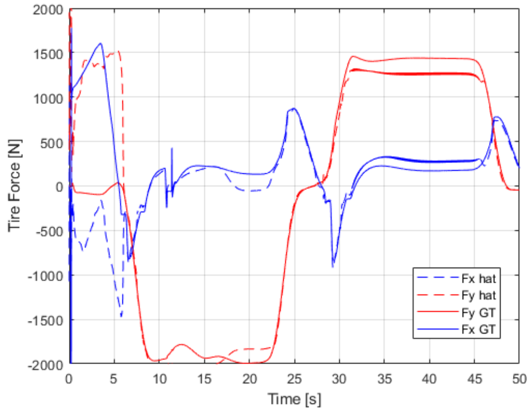

Figure 11: Tire force estimation (μ=0.8)

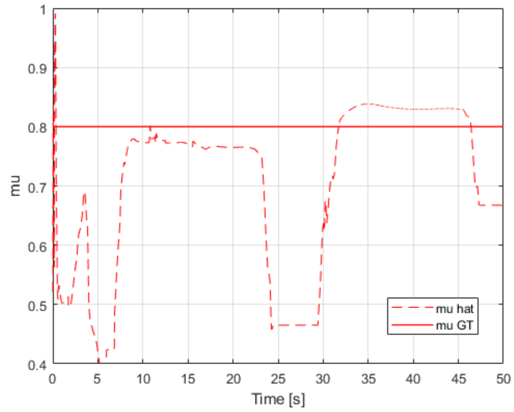

Figure 12: TRFC etimation (μ=0.8)

The estimation results for the longitudinal velocity (V_x), lateral velocity (V_y), and yaw rate (γ) are shown in Figures 9 and 10. The longitudinal velocity (V_x) was accurately estimated across the entire track, with minimal deviation even in curved sections. In contrast, slight fluctuations were observed in the lateral velocity (V_y) and yaw rate (γ) during high-curvature maneuvers, while the overall estimation trends were reasonably maintained.

5.2.2 Case 2: Low-mu ($\mu = 0.4$) test results

The vehicle was driven at a target speed of 40 km/h on a track composed of straight and curved sections under a low-mu surface ($\mu = 0.4$). Figures 13–16 present the estimation results for longitudinal and lateral velocities, yaw rate, tire forces, and TRFC.

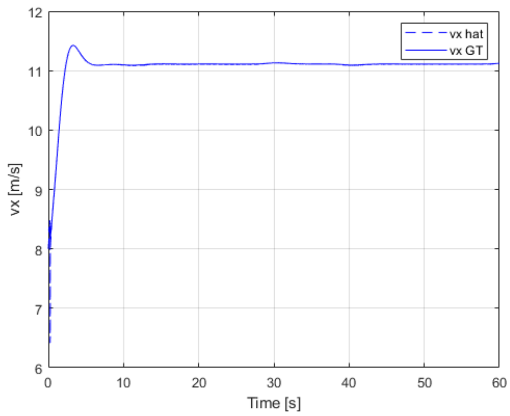

Figure 13: Longitudinal velocity(Vx) estimation (μ=0.4)

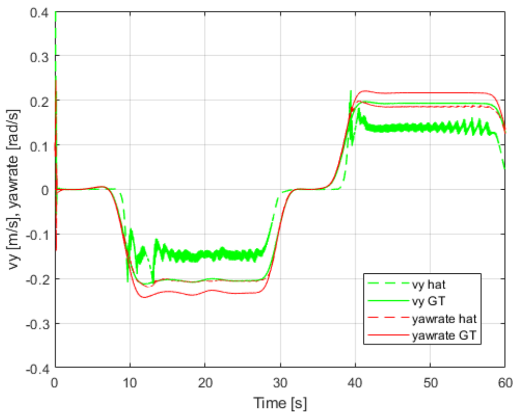

Figure 14: Lateral velocity(Vy) and yawrate(γ) etimation (μ=0.4)

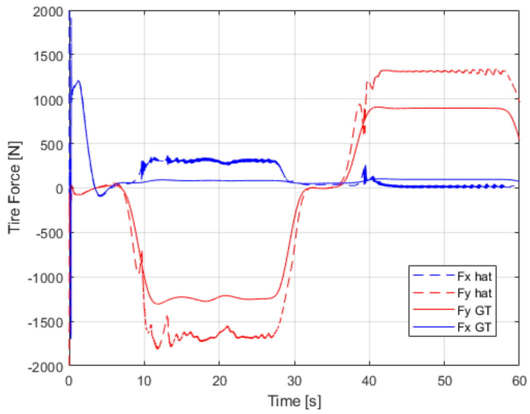

Figure 15: Tire force estimation (μ=0.4)

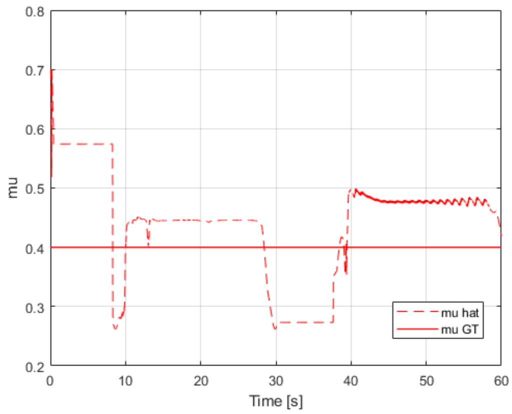

Figure 16: TRFC etimation (μ=0.4)

The estimation results for the longitudinal velocity (V_x), lateral velocity (V_y), and yaw rate (γ) under the low-mu ($\mu = 0.4$) condition are shown in Figures 13 and 14. The longitudinal velocity (V_x) was generally estimated with high accuracy throughout the test, although slight deviations were observed during transient phases such as acceleration and deceleration. For the lateral velocity (V_y) and yaw rate (γ), larger fluctuations were observed compared to the high-mu case, particularly during curved sections, owing to the reduced tire-road friction. Nevertheless, the overall trends in V_y and γ were reasonably captured despite the low-friction environment.

5.3 Discussion

Several factors contributed to the observed estimation errors, particularly under low-mu conditions. First, even in pure slip scenarios, the force fitting performance of the non-pneumatic tire (NPT) was less accurate in low slip regions. In these regions, the predicted tire forces tended to be either overestimated or underestimated, depending on the slip magnitude, which introduced discrepancies in force estimation. Such fitting errors were further amplified under combined slip conditions, where the Magic Formula model struggled to capture the coupled slip dynamics of NPT.
Moreover, the Cubature Kalman Filter (CKF)-based state estimation exhibited degraded performance under low friction surfaces. Specifically, inaccuracies in the longitudinal force (F_x) estimation, due to both model fitting errors and increased process noise under low-mu conditions, led to further deterioration in the overall TRFC estimation.
Additionally, the fitted tire model showed limited variation in force curvature characteristics with respect to vertical load changes. This lack of distinct curvature behavior made it challenging for the neural network to learn and differentiate the friction conditions based on normalized tire forces, resulting in reduced TRFC estimation accuracy across different vertical loads.
Overall, the combination of tire force fitting errors in low slip regions, degraded CKF-based state estimation in low-mu conditions, and limited curvature variation across vertical loads contributed to the challenges observed in TRFC estimation performance.

6 Conclusion

This study proposed a simulation-based framework for modeling and estimating the behavior of non-pneumatic tires (NPTs). A modified Magic Formula tire model was optimized using a Genetic Algorithm (GA) to capture the force characteristics of NPTs, and a Cubature Kalman Filter (CKF)-based state estimator combined with a machine learning regression model was developed to estimate tire-road friction coefficients (TRFC) during vehicle operation. This framework enables not only efficient evaluation of

NPT-equipped vehicles but also facilitates the development and validation of control strategies within simulation environments, minimizing the reliance on costly physical prototyping.
Simulation results demonstrated that the proposed method could accurately estimate vehicle states and TRFC under high-friction conditions. However, under low-friction and combined slip conditions, estimation errors increased due to tire model fitting limitations and reduced robustness in state estimation performance. These findings highlight the need for further improvements, particularly the development of tire force models tailored to NPT-specific characteristics and the design of estimation frameworks capable of maintaining robustness across a wide range of friction conditions.
Despite these limitations, the proposed methodology provides a foundational step toward simulation-based development of NPT vehicle dynamics and control systems, offering a promising direction for future research.

Acknowledgments

This work was supported by the National Research Foundation of Korea(NRF) grant funded by the Korea government(MSIT) (RS-2025-00522790), also this work was supported by the Technology Innovation Program (20013794, Center for Composite Materials and Concurrent Design) funded By the Ministry of Trade, Industry & Energy(MOTIE, Korea)

References

[1] L. Zhu, T. Xu, X. Liu, M. Wu, X. Zhou, and F. Gao, “Test and simulation study on the static load and pure longitudinal slip characteristics of non-pneumatic tire,” *Machines*, vol. 11, p. 86, 2023.

[2] L. Ku, H. Fu, K. Chen, J. Zhang, S. Bi, and L. Zhou, “Numerical analysis of steady-state mechanical characteristics of the flexible spoke non-pneumatic tire under multiple working conditions,” *Journal of Terramechanics*, vol. 106, pp. 35–45, 2023.

[3] Y. Wang, J. Hu, F. Wang, H. Dong, Y. Yan, Y. Ren, C. Zhou, and G. Yin, “Tire road friction coefficient estimation: Review and research perspectives,” *Chinese Journal of Mechanical Engineering*, vol. 35, no. 6, 2022.

[4] Y. Sun and Q. Chen, “Joint estimation of states and parameters of vehicle model using cubature kalman filter,” in *2016 IEEE International Conference on Systems, Man, and Cybernetics (SMC)*. IEEE, 2016, pp. 977–982.

[5] Y. Wang, G. Yin, P. Hang, J. Zhao, Y. Lin, and C. Huang, “Fundamental estimation for tire road friction coefficient: A model-based learning framework,” *IEEE Transactions on Vehicular Technology*, 2024.

[6] S. Tao, Z. Ju, L. Li, H. Zhang, and W. Pedrycz, “Tire road friction coefficient estimation for individual wheel based on two robust pmi observers and a multilayer perceptron,” *IEEE Transactions on Vehicular Technology*, vol. 73, no. 9, 2024.

[7] Z. Bei, X. Chen, W. Zhao, and C. Wang, “A novel algorithm for tire-road friction coefficient estimation using adaptive backpropagation neural network,” in *International Conference on Intelligent Systems and Robotics (CISR 2024)*, vol. 2832. IOP Publishing, 2024, p. 012018.

[8] H. B. Pacejka and E. Bakker, “The magic formula tyre model with transient properties,” *Vehicle System Dynamics*, vol. 27, no. Supplement, pp. 234–249, 1997.

[9] I. Arasaratnam and S. Haykin, “Cubature kalman filters,” *IEEE Transactions on Automatic Control*, vol. 54, no. 6, pp. 1254–1269, 2009.

[10] B. Leng, D. Jin, L. Xiong, X. Yang, and Z. Yu, “Estimation of tire-road peak adhesion coefficient for intelligent electric vehicles based on camera and tire dynamics information fusion,” *Mechanical Systems and Signal Processing*, vol. 150, p. 107275, 2021.

Presenter Biography

DongWook Cho received a B.S. degree in Mechanical Engineering from Sungkyunkwan University, Suwon, Korea, in 2024. He is currently studying for the M.S. degree in Intelligent Robotics at Sungkyunkwan University. His research interests include vehicle dynamics, state estimation, vehicle motion control, electric vehicles.

Hyunuk Lee received a B.S. degree in Aerospace Engineering from Korea Aerospace University, Goyang, Korea, in 2023. He is currently studying for the M.S. degree in Intelligent Robotics at Sungkyunkwan University. His research interests include torque vectoring, 4wheel-independent drive electric vehicles, vehicle models, virtual simulation.

Jeonghyuk Kim received a B.S. degree in Mechanical Engineering from Ajou University, Suwon, Korea, in 2023. He is currently studying for the M.S. degree in Mechanical Engineering at Sungkyunkwan University. His research interests include autonomous vehicle path planning and vehicle control.

Jiwon Im received a B.S. degree in Mechanical Engineering from Sungkyunkwan University, Suwon, Korea, in 2024. He is currently studying for the M.S. degree in Mechanical Engineering at Sungkyunkwan University. His research interests include sensor fusion, object detection, collision detection and autonomous vehicles.

Sung-Ho Hwang received his B.S., M.S., and Ph.D. degrees in Mechanical Design and Production Engineering from Seoul National University, Seoul, Korea, in 1988, 1990, and 1997, respectively. From 1992 to 2002, he worked as a Senior Researcher at the Korea Institute of Industrial Technology in Cheonan. Since 2002, he has been a Professor in the School of Mechanical Engineering at Sungkyunkwan University, Suwon, Korea. He has authored two books, published more than 100 articles, and holds over twenty patents. His research focuses on automotive mechatronics systems of electrified vehicles and control strategies for autonomous vehicles. Prof. Hwang served as Editor-in-Chief of the Journal of Drive and Control from 2012 to 2016 and is currently serving as President of KSAE (The Korean Society of Automotive Engineers) in 2025.